Interactions Contributing to the Tyrosyl Circular Dichroism Bands of Ribonuclease S and A†

E. Hardin Strickland

ABSTRACT: The near-ultraviolet circular dichroism (CD) bands of ribonuclease (RNase) S and A are examined theoretically by using the coordinates of crystalline bovine pancreatic RNase S. The tyrosyl CD is assumed to arise principally from coupling between the near-ultraviolet (^1L_b) tyrosyl band and the π–π^* transitions located on other moieties. The calculated tyrosyl CD bands give about 70% of the CD observed for RNase S at 275 nm. The remaining CD is attributed mainly to a negative disulfide band having its extremum located below 270 nm. Part of the disulfide CD results from the inherent dissymmetry of the four disulfide bridges in RNase S. Most of the tyrosyl rotatory strength arises from interactions between Tyr-73 and Tyr-115; *i.e.*, the far-ultraviolet aromatic transitions of each tyrosyl couple with the ^1L_b transition of the other. In addition, coupling between their ^1L_b transitions causes a small exciton CD component, which affects the shape of the spectrum. Smaller exciton CD components result from interactions between tyrosyl pairs 92–97 and 25–97. A portion of the total tyrosyl rotatory strength arises from coupling with the peptide transition at 190 nm. In the case of RNase S, the rotatory strength calculated for Tyr-25 is small. The calculations suggest, however, that an altered orientation of the Tyr-25 side chain may give a strong CD band due to coupling with the aromatic transitions of Phe-46 and His-48. Such a conformation change could account for the negative CD band (288.5 nm) given by Tyr-25 in RNase A.

Extensive vibronic structure has been observed in the near-ultraviolet CD[1] and absorption spectra of RNase S and A (Horwitz *et al.*, 1970; Horwitz and Strickland, 1971). By comparing the vibronic structure of these proteins to that found for tyrosyl model compounds, the approximate CD contributions of the tyrosyl and cystinyl side chains were estimated. In the RNase A spectrum between 275 and 310 nm, about 40–50% of the CD strength has been attributed to disulfide, 45–35% to the three tyrosyl residues with exposed hydroxy groups, and 20–15% to a single buried tyrosyl residue (Tyr-25). The CD spectrum of RNase S is similar except that Tyr-25 seems to have lost much of its CD intensity and has its absorption band shifted to shorter wavelengths.

Investigations using both crystals and solutions indicate that the hydroxy groups of Tyr-73, -76, and -115 are free to interact with the solvent (Wyckoff *et al.*, 1970; Richards and Wyckoff, 1971; Woody *et al.*, 1966; Li *et al.*, 1966). Tyr-97 is completely buried and has its hydroxy group hydrogen bonded to the carbonyl oxygen of Lys-41 (Richards and Wyckoff, 1971). The hydroxy group of Tyr-92 is hydrogen bonded to the carbonyl oxygen of Lys-37. Tyr-25, which is mostly buried in RNase S, has its hydroxy group hydrogen bonded to a carboxylate oxygen of Asp-14. In crystalline RNase A the environment of Tyr-25 may be somewhat different, since it is located close by the single peptide bond that is selectively cleaved by subtilisin (Wyckoff *et al.*, 1967).

Recently Chen and Woody (1971) and Hooker and Schellman (1970) have described theoretical studies on the CD bands of tyrosine compounds. Certain aspects of their techniques may be used to calculate the tyrosyl CD bands in proteins. Their results, together with studies on heme proteins (Hsu and Woody, 1971), suggest that electric dipole–electric dipole coupling may be the major source of tyrosyl CD bands in proteins. The near-ultraviolet transition of each tyrosyl side chain may couple with the strong far-ultraviolet transitions of other nearby moieties. Strong coupling interactions may be expected primarily with aromatic amino acids, peptide bonds, and other groups having π orbitals.

This communication describes a theoretical analysis of the near-ultraviolet tyrosyl CD bands of RNase S, based upon electric dipole–electric dipole coupling. To obtain the necessary atomic coordinates, the conformation of RNase S in solution and in glasses at 77°K is assumed to be identical with that reported for the crystalline state (Richards and Wyckoff, 1971). These calculations have revealed several interactions which give major tyrosyl CD bands. From this information, it is possible to identify conformation changes which may measurably affect the near-ultraviolet CD spectrum of RNase S. The interactions of Tyr-25 are examined in detail, because its CD bands are altered in RNase A. Some consideration is also given to possible static perturbations of tyrosyl side chains and to the inherent optical activity of the disulfide bridges.

Methods and Theoretical Considerations

The mechanisms giving rise to optical activity have been derived in detail by Tinoco (1962) and summarized by Schellman (1968). When an optically inactive chromophore is placed in a dissymmetric environment, CD bands may arise from one or more of the following mechanisms: (A) electric dipole–electric dipole coupling (nondegenerate or degenerate), (B) static perturbations (one-electron mechanism), and (C) electric dipole–magnetic dipole coupling ($\mu \cdot m$). In each of these mechanisms the chromophore gains CD by means of interactions (either static or dynamic) with the other moieties in the protein. Attention will be focused primarily upon the

† From the Laboratory of Nuclear Medicine and Radiation Biology, University of California, Los Angeles, California 90024. *Received April 10, 1972.* This work was supported by Contract AT(04-1) GEN-12 between the Atomic Energy Commission and the University of California.

[1] Abbreviations used are: CD, circular dichroism; $\Delta\epsilon$, ϵ for left circularly polarized light minus that for right circularly polarized light; RNase A, bovine pancreatic ribonuclease; RNase S, subtilisin-modified RNase A.

TABLE I: Characteristics of π-π^* Transitions in Various Chromophoric Groups.

Chromophoric Group	Excited State	λ^a (nm)	$\mu^b \times 10^{18}$ (cgs units)	$q_n{}^c$
Phenolic ring of Tyr	^1L_b	277	1.2[d]	*e*
	^1L_a	227	2.45	
	^1B_b	192	4.74	
	^1B_a	192	4.68	
Phenyl ring of Phe	^1B_b	189	4.5	*f*
	^1B_a	189	4.5	
Peptide bond	NV_1	190	3.05	*g*
	NV_2	125	1.7	
Side-chain amides of Gln and Asn	NV_1	181[h]	2.75[h]	*g*
Carboxylate of Glu and Asp	NV_1	173[i]	2.6[i]	*g*
Imidazolyl ring of His (uncharged)	1	210	2.4[j]	*f*
	2	210	1.1[j]	
	3	164[j]	3.8[j]	
	4	155[j]	1.6[j]	
Guanidino group of Arg	1	~170[k]	3–5[k]	*l*
	2	~170[k]	3–5[k]	*l*

[a] λ, wavelength. The spectra are shown in McDiarmid (1965) and Gratzer (1967). [b] μ, transition moment. In the calculations μ was obtained from the individual monopoles and their coordinates: $\boldsymbol{\mu} = \Sigma_n q_n x_n \hat{i} + \Sigma_n q_n y_n \hat{j} + \Sigma q_n z_n \hat{k}$ where the summation is made over all the monopoles for a specific transition. Monopole values were scaled by a multiplicative factor so that the calculated μ had value given in this table. [c] Reference for q_n, the transition monopoles. q_n were placed directly above and below the nuclear plane and centered on the nuclei; *i.e.*, the monopoles were placed in the region of the π orbitals. Unless indicated otherwise, the separations used were those derived by Woody (1968). At carbon atoms, ±1.08 Å; at nitrogen atoms, ±0.981 Å; at oxygen atoms, ±0.774 Å. Some calculations presented in Tables IV and VI used the monopole separations given by Nielsen and Schellman (1971). At C, ± 0.707 Å; at N, ±0.589 Å; at O, ±0.505 Å. [d] μ for ^1L_b tyrosyl band is taken from Hooker and Schellman (1970) and Strickland *et al.* (1972). [e] Chen and Woody (1971). [f] Hsu (1970). [g] These transition monopoles were calculated from the direction and magnitude of μ (Woody and Tinoco, 1967). [h] Average of values given by Nielsen and Schellman (1971). [i] Hooker and Schellman (1970). [j] Values are based upon theroetical calculations (Hsu, 1970). [k] Estimated from a partial spectrum of arginine (McDiarmid, 1965). [l] Approximate monopoles were calculated from the wave functions of the guanidinium ion (Paoloni, 1959) and scaled to give a dipole strength of 20×10^{-36} cgs unit. The transition intensities were then divided equally among the three orientations permitted by symmetry.

nondegenerate electric dipole–electric dipole coupling, because this mechanism seems best able to produce the intense tyrosyl circular dichroic bands observed in ribonuclease.

Electric Dipole–Electric Dipole Coupling (Nondegenerate). The method for calculating rotatory strength is similar to that used by Hsu and Woody (1971) for heme optical activity. The interactions between the near-ultraviolet tyrosyl transition and the transitions in other groups were considered pairwise using the equation

$$R_n = \frac{2\pi V_{12}\lambda_1\lambda_2}{hc(\lambda_2{}^2 - \lambda_1{}^2)}(\mathbf{R}_{21} \cdot \boldsymbol{\mu}_2 \times \boldsymbol{\mu}_1) \qquad (1)$$

where h = Planck's constant, c = velocity of light, V_{12} = the interaction energy between the two transitions, λ_1 = wavelength of the near-ultraviolet tyrosyl band (^1L_b), λ_2 = wavelength of the second transition, $\boldsymbol{\mu}_1$ = transition dipole moment of the ^1L_b band, located at center of phenolic ring, $\boldsymbol{\mu}_2$ = dipole moment of the transition coupling with $\boldsymbol{\mu}_1$ and is located at the center of second chromophore, $\mathbf{R}_{21} = \mathbf{R}_2 - \mathbf{R}_1$ = the distance from the center of the first tyrosyl ring to the center of the second chromophore.

I treated interactions of the ^1L_b transition from each tyrosyl residue with the far-ultraviolet π-π^* transitions of the following moieties: the aromatic side chains of Phe, His, and other Tyr; the amide groups of the peptide backbone and of side chains (Gln and Asn); the carboxylate ions; and the guanidino groups (Arg). The rotatory strength for the interactions between two groups was the summation of the individual interactions of the ^1L_b tyrosyl transition in residue one with each of the far-ultraviolet transitions in the second group.

The interaction energies in eq 1 were calculated using the point monopole approximation[2] (Woody, 1968; Hsu and Woody, 1971).

$$V_{12} = \sum_j \sum_k \frac{q_{2j}q_{1k}}{\epsilon_{2j1k}r_{2j1k}} \qquad (2)$$

where q_{1k} = kth monopole for the ^1L_b tyrosyl transition, q_{2j} = jth monopole for the transition in the other group, r_{2j1k} = distance between these monopoles, and ϵ_{2j1k} = dielectric constant at optical frequencies for the region between the monopoles. The summations included each ^1L_b monopole of the tyrosyl ring interacting with each monopole belonging to the other group. The transition monopoles and other characteristics of the chromophores may be obtained from the literature (Table I).

Note that the interaction energy eq 2 has a dielectric constant term in the denominator. I have taken the dielectric constant to be unity, in keeping with the assumptions made by others (Chen and Woody, 1971; Hooker and Schellman, 1970). This approximation seems satisfactory when the two chromophores are nearly in van der Waals contact. When other moieties lie between the two interacting chromophores, the dielectric constant should be set equal to the square of the index of refraction. This quantity cannot be determined precisely, though it probably lies between 1 and 2.5. Thus the calculated rotatory strengths are overestimated by an uncertain amount when the interacting groups have a large separation, *e.g.*, 10 Å. Evidently the rotatory strength falls off more rapidly with distance than the $1/R^2$ dependence expected for a dielectric constant of 1.

To be completely rigorous, the interactions of tyrosyl with the peptide bonds should be treated by matrix methods that take into account the simultaneous amide–amide interactions (Chen and Woody, 1971; Bayley *et al.*, 1969). Nevertheless, a pairwise treatment of the tyrosyl–amide interactions probably does not significantly increase the uncertainty in these cal-

[2] Since the dipole–dipole approximation is unreliable for small separations (Chen and Woody, 1971), it was not used to calculate V_{12}.

culations, because other uncertainties also exist. These include: the exact crystal structure of RNase S (see below), whether the structure is the same in solution and in the crystal, the separation of the transition monopoles above and below the nuclear plane (Table I), and the dielectric constant value.

Coupling of the tyrosyl ^1L_b transition with the σ–σ^* transitions was not calculated. These vacuum ultraviolet transitions are not well characterized. Furthermore, since each bond has a σ–σ^* transition, they tend to be distributed almost randomly around each phenolic ring. Thus their CD contributions are likely to cancel one another. In the case of heme CD bands, Hsu and Woody (1971) reported that coupling with the σ–σ^* transitions of alkyl groups is probably substantially smaller than coupling with the aromatic π–π^* transitions.

Degenerate Dipole–Dipole Coupling. The interaction between ^1L_b transitions on two different tyrosyl rings does not affect the net rotatory strength, but can alter the shape of the near-ultraviolet tyrosyl bands (Strickland *et al.*, 1970b). These degenerate interactions were calculated using the following equations (Tinoco, 1963; Schellman, 1968)

$$R_{s\pm} = \pm\frac{\pi}{2\lambda_1}(\mathbf{R}_{21}\cdot\boldsymbol{\mu}_2 \times \boldsymbol{\mu}_1) \tag{3}$$

$$\tilde{\nu}_\pm = \frac{1}{\lambda_1} \pm V_{12}/hc \tag{4}$$

where $R_{s\pm}$ = rotatory strengths of the two absorption bands centered at $\tilde{\nu}_+$ and $\tilde{\nu}_-$ wave numbers, respectively.

The exciton CD spectra were generated by summing the positive and negative components after splitting them by the calculated value (Strickland *et al.*, 1970b). The actual exciton CD spectra may be somewhat weaker. These calculations may overestimate the splitting, because strong coupling was assumed (Kasha, 1963). Actually the tyrosyl ^1L_b transition has intermediate intensity.

Static Perturbations. Schellman (1966) has described in detail the mechanism by which static perturbations may induce optical activity in a chromophore. The dipolar and ionic groups of a protein are the most effective perturbations. The amount of CD induced by these groups depends upon their geometry and upon the symmetry of the chromophore. Since the phenolic side chains have two symmetry planes (Horwitz *et al.*, 1970), the static perturbations are less effective than would be the case with a less symmetrical chromophore. If the perturbing group is an ion, the rotatory strength generated by the interaction decreases as $1/R^3$, where R is the distance from the center of the phenolic ring to the center of the other group. For dipolar perturbing groups, the distance dependence ($1/R^4$) is even steeper. Thus perturbing groups need to be practically in van der Waals contact to induce CD in the phenolic chromophore. In addition, a perturbing group cannot induce any CD if it lies in one of the two symmetry planes of the phenolic ring. These restrictions suggest that the static perturbation mechanism is less likely to induce major tyrosyl CD bands than is the dipole–dipole coupling mechanism. Nevertheless, polar groups near tyrosyl side chains in RNase S have been tabulated.

RNase S Crystal Data. Calculations were made using RNase S coordinates (set 6B, revised April 1971) kindly supplied by Professor Wyckoff and his coworkers. Preliminary calculations were carried out with the coordinates published by Wyckoff *et al.* (1970). The interactions between aromatic moieties were not much changed by refinement of the RNase S coordinates. In contrast, the total rotatory strengths calculated for the tyrosine–peptide bond interactions were altered, especially for Tyr-92.

Computations revealed that the bond lengths obtained from the RNase S crystal data sometimes deviated by more than ±0.1 Å from the standard dimensions observed in the X-ray studies of amino acids and small peptides. No attempt was made to give each residue the standard bond lengths, even though these deviations may cause some error in the calculated rotatory strength. Instead the error was partially eliminated by correcting the rotatory strength in the following way. The sizes of the monopoles for each transition were scaled by a constant fraction so that the resulting dipole moment for each residue gave the experimental value listed in Table I.

Some interpretation of the crystal data was required before interactions with the four histidinyl residues could be evaluated. The X-ray data on RNase S do not distinguish between the nitrogen and carbon atoms of the imidazolyl rings. Tentative assignments can be made, however, by using the hydrogen-bonding scheme proposed by Richards and Wyckoff (1971). Any imidazolyl atom bonded to a hydrogen acceptor atom in an adjacent moiety must be a >NH group. Specific atoms in the list of atomic coordinates were identified by calculating the distances from each imidazolyl atom to the designated hydrogen acceptor atom. The hydrogen-bonded nitrogen atom was clearly distinguished by its short separation (about 2.4–3.0 Å) from the hydrogen acceptor atom. Each imidazolyl ring appears to have only a single bond to a hydrogen acceptor atom belonging to RNase S. Thus the other imidazolyl nitrogen atom was assumed to have different degrees of protonation, depending upon the pH. Judging from the pK values of the histidinyl side chains (Meadows *et al.*, 1968), the second imidazolyl nitrogens are more than half-protonated in RNase S used for the X-ray studies (crystals grown at pH 5.9–6.0). The rotatory strength calculations must be based upon coupling with the unprotonated imidazole ring, because no transition monopoles are available for the protonated form.

Results

Nondegenerate Electric Dipole–Electric Dipole Coupling between Tyrosyls. Coupling of the tyrosyl ^1L_b transition in each residue with the far-ultraviolet transitions of the other tyrosyl side chains is summarized in Table II. Only the interactions between Tyr-73 and Tyr-115 produce a large rotatory strength (total of about -7×10^{-40} cgs unit). The other pairs of tyrosyl side chains are too far apart (10 Å or more) to give much rotatory strength.

Coupling of Tyrosyl and Phenylalanyl Transitions. None of these interactions contribute significantly to the rotatory strength of RNase S. Nevertheless, the interactions between Tyr-25 and Phe-46 are of interest due to the proximity of their side chains (6.5 Å between centers). The net rotatory strength is small only because the two individual interactions have opposite signs (Table II). Coupling of the ^1L_b transition in Tyr-25 with the ^1B_b band in Phe-46 gives $+1.2 \times 10^{-40}$ cgs unit, whereas coupling with the ^1B_a band gives -1.4×10^{-40} cgs unit.

Coupling of Tyrosyl and Histidinyl Transitions. With one exception, the histidinyl side chains are too far from the phenolic rings to give much rotatory strength (Table III). The imidazolyl ring of His-48, however, is in van der Waals con-

TABLE II: Near-Ultraviolet Tyrosyl Rotatory Strength Resulting from Coupling with Transitions in Other Tyrosyl and Phenylalanyl Side Chains of RNase S.

		Tyrosyl Side Chain											
		73		115		76		25		92		97	
μ_2[a]		R_{21}[b] (Å)	$R_s \times 10^{40}$ (cgs)	R_{21} (Å)	$R_s \times 10^{40}$ (cgs)	R_{21} (Å)	$R_s \times 10^{40}$ (cgs)	R_{21} (Å)	$R_s \times 10^{40}$ (cgs)	R_{21} (Å)	$R_s \times 10^{40}$ (cgs)	R_{21} (Å)	$R_s \times 10^{40}$ (cgs)
Tyr-73	^1L_a			6.0	−1.4	10	0.1	27	0	36	0	29	0
	^1B_b				0.4		0		0.1		0		0.1
	^1B_a				−2.5		0.1		−0.1		0		−0.1
Tyr-115	^1L_a	6.0	−1.5			15	0	29	0	35	0	30	0
	^1B_b		0.3				0.1		0		0		0
	^1B_a		−2.6				0		0		0		0
Tyr-76	^1L_a	10	−0.1	15	−0.1			27	0	40	0	32	0
	^1B_b		0.1		0.1				0		0		0
	^1B_a		0.1		−0.2				−0.1		0		−0.1
Tyr-25	^1L_a	27	0	29	0	27	0			20	0	11	0.2
	^1B_b		0.1		0		0				−0.1		−0.1
	^1B_a		0		0		0				0		0.4
Tyr-92	^1L_a	36	0	35	0	40	0	20	0.1			11	0
	^1B_b		0		0		0		−0.1				0.5
	^1B_a		0		0		0		0.1				0.1
Tyr-97	^1L_a	29	0	30	0	32	0	11	0.3	11	−0.2		
	^1B_b		0.1		0		0		−0.1		0.4		
	^1B_a		0		0		0		0.5		−0.3		
Phe-8	^1B_b	12	0.2	12	0.4	17	−0.1	17	0.1	25	0	18	0.2
	^1B_a		0.1		−0.4		0		−0.2		0		−0.1
Phe-46	^1B_b	23	−0.1	24	0	25	0.1	6.5	1.2	18	−0.1	9.5	−0.3
	^1B_a		0		0		0		−1.4		0.1		−0.3
Phe-120	^1B_b	14	0	16	0.2	17	−0.1	15	0	24	0	16	0.1
	^1B_a		−0.1		−0.1		0.1		−0.2		0		0
Total $R_s \times 10^{40}$			−3.6		−3.6		0.3		−0.1		−0.1		0.5

[a] μ_2, transition in second chromophore that couples with the ^1L_b tyrosyl transition. [b] R_{21}, distance from tyrosyl ring center to other chromophoric center.

tact with the phenolic oxygen[3] of Tyr-25. This interaction gives a calculated rotatory strength of -1.3×10^{-40} cgs unit.

Coupling of Tyrosyl and Peptide Transitions. The rotatory strengths for coupling between the tyrosyl ^1L_b band and the NV_1 transition in a single peptide bond vary both in magnitude and in sign (Figures 1 and 2). When the moieties are nearly in contact (4–5 Å between centers), the absolute magnitude of the rotatory strength sometimes exceeds 1×10^{-40} cgs unit. Most interactions, however, give less than $\pm 1 \times 10^{-40}$ cgs unit. For separations exceeding 10 Å, the absolute magnitude of the rotatory strength is below 0.3×10^{-40} cgs unit.

The total rotatory strength for each phenolic ring is obtained by summing the individual interactions. These values vary from 1.8×10^{-40} cgs unit for Tyr-76 to -2.4×10^{-40} cgs unit for Tyr-97 (Table IV)

In the case of Tyr-76, the calculated rotatory strength is significantly influenced by the choice of monopole separations above and below the nuclear plane (Table IV). For the strong interaction between Tyr-76 and peptide bond 60, the smaller separation used by Nielsen and Schellman (1971) gives 30% less rotatory strength than does the larger separation used by Woody (1968). In general, the two separations may yield somewhat different rotatory strengths when the interacting groups are approximately in contact. For groups not in contact, the choice of separations is not so important. With the exception of the Tyr-76 peptide interactions, the sums of all peptide interactions give rotatory strengths that are similar for either the large or the small monopole separations (Table IV).

Calculations were also made of coupling between the peptide NV_2 transition (125 nm) and the tyrosyl ^1L_b transition. These interactions do not contribute measurable rotatory strength.

Tyrosyl Coupling with Transitions of Other Groups. The guanidino groups of the four argininyl side chains are all more than 8 Å away from the phenolic rings. Calculations indicated that these coupling interactions are too small to give measureable rotatory strengths.

Among the 12 carboxylate groups, only Asp-14 and Glu-86 are close by phenolic rings. Even in these cases, the calculated rotatory strengths are small (Table V). In addition, the carboxylate group of Glu-86 is poorly defined in the electron-

[3] See Figure 4F in Wyckoff *et al.* (1970) for approximate orientation. Richards and Wyckoff (1971) have revised the hydrogen-bonding scheme so that a carbon atom of the imidazolyl ring contacts the phenolic oxygen.

TABLE III: Near-Ultraviolet Tyrosyl Rotatory Strength Resulting from Coupling with Transitions in Histidinyl Side Chains of RNase S.

	Tyrosyl Side Chain											
	73		115		76		25		92		97	
μ_2 on[a]	R_{21}[b] (Å)	$R_s \times 10^{40}$ (cgs)	R_{21} (Å)	$R_s \times 10^{40}$ (cgs)	R_{21} (Å)	$R_s \times 10^{40}$ (cgs)	R_{21} (Å)	$R_s \times 10^{40}$ (cgs)	R_{21} (Å)	$R_s \times 10^{40}$ (cgs)	R_{21} (Å)	$R_s \times 10^{40}$ (cgs)
His-12	16	−0.1	17	0.1	20	0	14	0.1	20	0	13	0.1
His-48	22	0	24	0	21	0	5.7	−1.3	24	0	15	−0.1
His-105	15	0.1	20	0.1	9.1	0	21	0	36	0	26	0
His-119	11	0	12	−0.1	19	0	22	0.1	25	0	20	0.1
Total $R_s \times 10^{40}$		0.1[c]		0[c]		0		−1.1		0		0[c]

[a] μ_2 on, chromophoric group whose transitions couple with the ^1L_b tyrosyl transition. [b] R_{21}, distance between ring centers. [c] Apparent discrepancy of total R_s value from sum of individual R_s values results from errors caused by rounding off individual values.

density maps (Wyckoff *et al.*, 1970), suggesting that it may have motility, which further reduces its effective coupling.

There are three close interactions with side-chain amides: Asn-62 with Tyr-73, Gln-60 with Tyr-76, and Asn-27 with Tyr-97. Judging from their contours in the electron density maps, these amides are relatively rigid in crystalline RNase S (Wyckoff *et al.*, 1970). Both Asn-27 and Gln-60 are hydrogen bonded, which permits their oxygen and nitrogen atoms to be distinguished. In the case of Asn-62 either the O^{δ_1} or the N^{δ_2} atom contacts the C^{ϵ_1} atom of Tyr-73. Owing to the strong permanent dipole moment of amides, the most probable orientation seems to be with the NH_2 group nearest the π orbitals of the phenolic ring. In spite of the proximity of these side-chain amides to tyrosyl residues, the summations of their dipole–dipole couplings give rotatory strengths of less than $\pm 0.3 \times 10^{-40}$ cgs unit/tyrosyl, if the N^{δ_2} atom of Asn-62 contacts the ring of Tyr-73. Even if the O^{δ_1} atom (Asn-62) is nearest the ring, the rotatory strength of Tyr-73 increases by only 0.3×10^{-40} cgs unit (Table V).

Degenerate Dipole–Dipole Coupling (Exciton). The sizes of the exciton CD spectra resulting from coupling between the ^1L_b tyrosyl bands may be evaluated from the $\Delta\epsilon$ values summarized in Table VI. The interaction between Tyr-73 and Tyr-115 causes the largest exciton CD component ($\Delta\epsilon_{max}$ 0.56 M^{-1} cm^{-1}). Smaller exciton effects result from the tyrosyl pairs 92–97 and 25–97.

Static Perturbations. Each of the tyrosyl side chains is located close by at least several polar groups in RNase S (Ta-

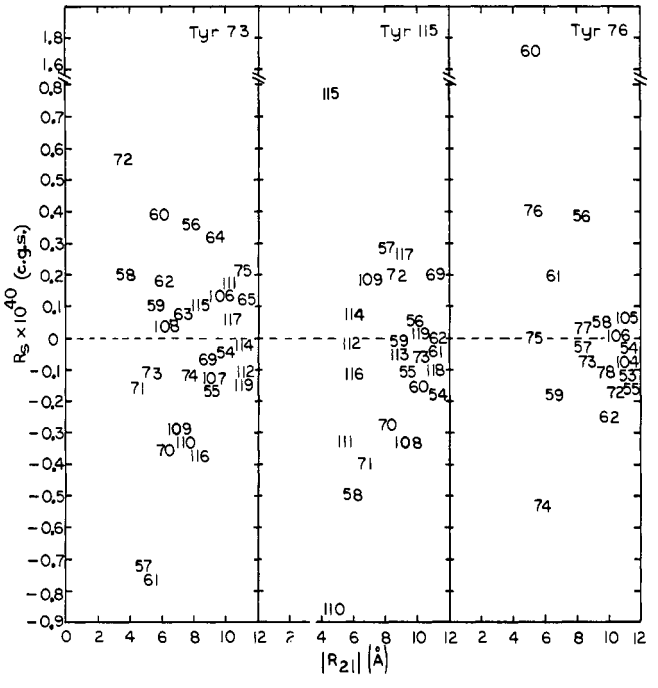

FIGURE 1: Dependence of rotatory strength (R_s) upon distance ($|R_{21}|$) for coupling the ^1L_b transitions of Try-73, -115, and -76 with the π–π^* peptide transitions at 190 nm. The values for these interactions (up to 12 Å) are plotted using a number to designate which peptide bond is involved. This number corresponds to the residue providing the C atom for the peptide linkage.

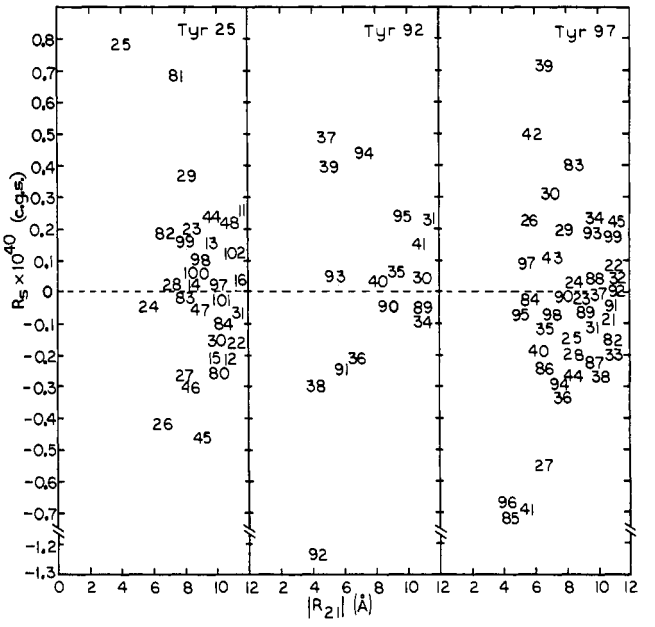

FIGURE 2: Distance dependence for coupling of the ^1L_b tyrosyl transitions of Tyr-25, -92, and -97 with the peptide π–π^* transitions at 190 nm.

TABLE IV: Effect of Monopole Position in π Orbital upon the Calculated Rotatory Strength of near-Ultraviolet Tyrosyl Bands.

	$R_s \times 10^{40}$ for Tyrosyl Side Chains (cgs)											
	73		115		76		25		92		97	
All Interactions with	L[a]	S[b]	L[a]	S[b]	L[a]	S[b]	L[a]	S[b]	L[a]	S[b]	L[a]	S[b]
Other Tyr side chains	−3.7	−4.0	−3.7	−3.9	0.4	0.4	0.5	0.4	−0.1	−0.1	0.9	0.9
Phe side chains	0.1	0.1	0.1	0.1	−0.1	−0.1	−0.5	−0.7	0	0	−0.5	−0.4
Peptide bonds (NV_1)	−1.3	−1.4	−1.5	−1.3	1.8[c]	1.4[c]	0.6	0.5	−0.4	−0.2	−2.4	−2.3
His side chains	0.1	0.1	0	0	0	0	−1.1	−1.1	0	0	0	0
Total $R_s \times 10^{40}$	−4.8	−5.2	−5.1	−5.1	2.1	1.7	−0.5	−0.9	−0.5	−0.3	−2.0	−1.8

[a] L, monopoles separated from the nuclear plane by larger distances used by Woody (1968). See Table I. [b] S, monopoles separated from the nuclear plane by smaller distances used by Nielsen and Schellman (1971). [c] This difference results primarily from the different interactions with peptide bond 60.

TABLE V: Moieties Having Either Strong Dipole–Dipole Couplings or Small Separations from the Tyrosyl Side Chains of RNase S.

μ_2 on[a]	r_{min}[b] (Å)	R_{21}[c] (Å)	R_s[d] $\times 10^{40}$ (cgs)
	Tyr-73		
Tyr-115	3.0	6.0	−3.9
Asn-62	1.3	4.3	0.3[e] or 0.6
PB[h]-57	3.2	5.0	−0.7
PB-58	1.3	3.7	0.2
PB-59	2.7	5.6	0.1
PB-60	3.2	5.7	0.4
PB-61	3.0	5.4	−0.8
PB-71	2.1	4.7	−0.2
PB-72	1.0	3.6	0.6
Cys-58–110	3.0[f]		
	Tyr-115		
Tyr-73	2.7	6.0	−3.5
PB-58	3.3	5.9	−0.5
PB-110	1.8	4.5	−0.9
PB-111	2.7	5.3	−0.3
PB-115	2.2	4.4	0.8
Cys-58–110	2.7[f]		
	Tyr-92		
PB-37	2.8	4.9	0.5
PB-38	1.6	4.3	−0.3
PB-39	2.7	5.1	0.4
PB-92	1.7	4.3	−1.2
	Tyr-76		
Gln-60	2.2	5.0	−0.1
PB-60	2.4	4.8	1.7
PB-74	3.4	5.9	−0.5
PB-75	2.2	5.3	0
	Tyr-25		
Phe-46	3.4	6.5	−0.2
His-48	3.6	5.7	−1.3
Asp-14	3.6	5.6	0.2[g]
PB-25	1.6	4.0	0.8
PB-81	4.8	7.7	0.7
Met-29	3.3[f]	5.9	
Thr-82	2.7[f]	4.4	
	Tyr-97		
Glu-86	4.0	6.2	−0.2
Asn-27	3.2	5.6	−0.2
PB-26	3.0	5.5	0.2
PB-27	4.4	6.6	−0.6
PB-39	4.8	6.8	0.7
PB-41	2.9	5.4	−0.7
PB-42	3.6	5.9	0.5
PB-84	3.2	5.8	0
PB-85	2.7	4.8	−0.7
PB-95	2.5	5.1	−0.1
PB-96	2.3	4.3	−0.7
Met-30	1.4[f]	4.2	*g*
Thr-36	3.4[f]	4.9	
Cys-26–84	3.5[f]		
Cys-40–95	2.6[f]		

[a] μ_2 on, group interacting with the tyrosyl ^1L_b transition. PB designates peptide bond. Amino acid abbreviations designate the side chain of residue. [b] r_{min}, smallest separation between the ^1L_b tyrosyl monopoles and the second group's monopoles. (^1L_b monopoles are located on Cδ and Cϵ atoms of phenolic ring.) [c] R_{21}, distance between the centers of the two interacting groups. [d] R_s, tyrosyl rotatory strength from dipole–dipole coupling. [e] 0.3, for NH_2 nearest phenolic ring; 0.6, for >C = 0 nearest phenolic ring (see text). [f] Smallest separation between the tyrosyl monopoles and the heteroatom of the other amino acid side chain. [g] Perturbing group nearly lies in a symmetry plane of the phenolic ring. [h] PB = peptide bond.

TABLE VI: Exciton Circular Dichroism Bands of Tyrosyl Side Chains in RNase S.

Interacting Pair[a]	$\Delta\epsilon_1$[b] (M^{-1} cm^{-1})	$\Delta\epsilon_2$[c] (M^{-1} cm^{-1})	$R_{s\pm}$[d] $\times$ 10^{40} (cgs)	$\Delta\tilde{\nu}$[e] (cm^{-1})
73–115	0.56	0.36	$\mp$19.5	$\pm$14.6[f]
92–97	0.48	0.31	$\pm$42.7	$\mp$5.2
25–97	−0.10	−0.06	$\mp$15.4	$\mp$2.9

[a] Omitted pairs have negligible $\Delta\epsilon$ values. [b] Value at the longest wavelength peak. Band shapes are shown in Figure 3. [c] Value at the next peak having same sign as the longest wavelength peak. [d] $R_{s\pm}$, rotatory strengths of the two absorption bands split by $\pm\Delta\tilde{\nu}$. [e] $\Delta\tilde{\nu} = \pm V_{12}/hc$, splitting of degenerate ^1L_b bands, calculated using large monopole separations from nuclear plane (see Table I). [f] $\pm$9.8 cm^{-1} is obtained using small monopole separations.

TABLE VII: Inherent Optical Activity of the Disulfide Bonds of RNase S.

Cys	Dihedral Angle[a] (deg)	CD Sign of Longest λ Band[a]
26–84	−100.8 (−90 − 10.8)	+
65–72	104.4[b] (+90 + 14.4)	−
58–110	−84.6 (−90 + 5.4)	−
40–95	−84.6 (−90 + 5.4)	−

[a] Measured using the convention and diagram of Ludescher and Schwyzer (1971). Calculations based upon 1971 crystal data of Wyckoff and coworkers. [b] This angle is 20° greater than the value obtained using the earlier data of Wyckoff *et al.* (1970).

ble V). Mostly these polar groups are the moieties involved in dipole coupling with the ^1L_b tyrosyl transition. Tyr-97 and -73 contact numerous polar groups, which seem almost randomly distributed around their side chains. Probability considerations suggest that the rotatory strengths from static perturbations of these two phenolic rings would tend to cancel extensively. The side chain of Tyr-25 is in contact with both a carboxylate group (Asp-14) and an imidazolyl ring (His-48).[8] The carboxylate group of Asp-14, however, lies nearly in a symmetry plane of the phenolic ring, which precludes much rotatory strength from this perturbation. The rings of Tyr-92, -76, and -115 contact the fewest polar moieties.

Disulfide Bonds. The four disulfide groups of RNase S have dihedral angles that are near +90 or −90° (Table VII). By applying a quadrant rule, the sign for the inherent CD of each disulfide can be predicted from the dihedral angle (Ludescher and Schwyzer, 1971). The quadrants are bounded by the dihedral angles which do not give inherent optical activity (0, ±90, ±180°). Three of the four disulfide bonds of RNase S have inherent CD that is negative in the longest wavelength region (Table VII). The sign of the total CD inherent from all four disulfides can be determined by considering further the angular dependence of the inherent CD. For dihedral angles near ±90°, the absolute magnitude of the inherent CD increases as some function of the deviation from +90 or −90°. Evidently the positive CD band from Cys-26–84 (angle of −90° − 10.8°) is more than cancelled by the negative band of Cys-65–72 (angle of +90° + 14.4°). Since the other two cystinyl side chains have negative CD, the net CD contribution inherent from the dissymmetry of all four disulfides should be negative.

Discussion

Calculations of nondegenerate electric dipole–electric dipole coupling have revealed several interactions which contribute to the near-ultraviolet tyrosyl CD bands of RNase S. The largest interactions involve the side chains of Tyr-73 and Tyr-115, which are located close by each other. Their interactions give a calculated rotatory strength of about -7×10^{-40} cgs unit (Table V). The size of this calculated value lies within the range observed for model compounds containing two tyrosyl side chains located in promixity. For example, the near-ultraviolet rotatory strength of L-tyrosyl-L-tyrosyldiketopiperazine at 140°K is 6.6×10^{-40} cgs unit (Strickland *et al.*, 1970b).

Several of the other important coupling interactions in RNase S involve aromatic side chains near Tyr-25. Coupling the ^1L_b transition of Tyr-25 with the far-ultraviolet transitions of the imidazolyl moiety in His-48 gives a calculated rotatory strength of about -1×10^{-40} cgs unit (Table V). In addition, the interaction of Tyr-25 with the phenyl ring of Phe-46 is potentially important. Although these moieties are near each other, the calculated rotatory strength is small in RNase S (Table V). A local conformation change, however, could cause a major tyrosyl CD band to arise from the interaction of Tyr-25 with the side chain of Phe-46. In RNase A, Tyr-25 does have a measurable negative CD band at 288.5 nm (Horwitz *et al.*, 1970). Probably the 288.5-nm CD band of RNase A results at least partly from the interactions of Tyr-25 with the aromatic side chains of Phe-46 and His-48.

The CD of RNase S arises also from the ^1L_b tyrosyl transitions coupling with the NV_1 transitions of the peptide bonds. Most of the tyrosyl interactions with a single peptide bond give rotatory strengths whose absolute magnitudes are less than 1×10^{-40} cgs unit. The interaction between Tyr-76 and peptide bond 60, however, may be as large as 1.7×10^{-40} cgs unit (Table V). This range of values is comparable to that observed for tyrosyl compounds with a single aromatic side chain and with one to two amide or ester linkages (Strickland *et al.*, 1970b, 1972). Apparently the rotatory strengths calculated for tyrosyl interactions with single peptide bonds in RNase S have approximately the correct size. This agreement lends support to the validity of the dipole–dipole coupling calculations.

The rotatory strengths for tyrosyl coupling with all peptide bonds vary from about 2×10^{-40} to -2×10^{-40} cgs unit per tyrosyl (Table IV). This range is only slightly larger than that calculated for coupling with a single peptide bond. In spite of the numerous peptide groups surrounding some tyrosyls, *e.g.*, Tyr-97, the total rotatory strengths are held down by cancellation of contributions having opposite signs (Figures 1 and 2).

Evidently the relative sizes of the different coupling interactions in RNase S are similar to those reported to occur in poly(L-tyrosine) (Chen and Woody, 1971). Most of the near-

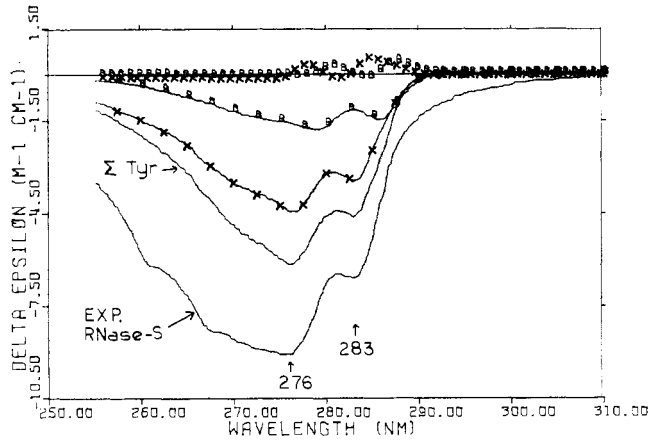

FIGURE 3: Comparison between the tyrosyl CD bands calculated for RNase S and the CD spectrum observed for RNase S at 77°K. The experimental trace (EXP RNase S) is taken from Horwitz and Strickland (1971). ΣTyr, sum of the individual tyrosyl CD bands and their exciton components; X–X, CD spectrum of Tyr-73, -115, and -76 obtained by converting their rotatory strengths (Table IV); B—B, CD spectrum of Tyr-25, -92, and -97; X X X, exciton CD component for Tyr-73–115 interaction; B B B, exciton CD component for sum of Tyr-25–97 and Tyr-92–97 interactions (Table VI). The shapes of the calculated CD contributions were determined from the tyrosyl spectra of model compounds (Horwitz *et al.*, 1970; Strickland *et al.*, 1970b, 1972). For Tyr-73, -76, and -115, the CD spectrum was assumed to have the same shape as that of L-tyrosine in water–glycerol (1:1, v/v) at 77°K ($\Delta\epsilon$ at 277 nm = $0.56 \times R_s \times 10^{40}$). For Tyr-25, -92, and -97, the shape was taken from the CD spectrum of L-tyrosine ethyl ester in ether–pentane–alcohol (5:5:2, v/v) at 140°K ($\Delta\epsilon$ at 279.5 nm = $0.60 \times R_s \times 10^{40}$).

ultraviolet tyrosyl CD arises from coupling with the far-ultraviolet π–π^* transitions of aromatic side chains, but some also results from coupling with the peptide π–π^* transition at 190 nm.

Next I shall compare the tyrosyl CD spectrum calculated from dipole–dipole coupling with the CD spectrum observed for RNase S under appropriate experimental conditions. First, note that the tyrosyl side chains appear to be relatively rigid in RNase S, since the rotatory strength measured from 250 to 310 nm (pH 7) is nearly identical at 297°K and below (Horwitz and Strickland, 1971). Secondly, due to better resolution of the vibronic structure at low temperatures, the 77°K CD spectrum of RNase S provides the most rigorous test for the calculated spectrum. Thirdly, the wavelength positions of the individual tyrosyl CD spectra should be selected in accordance with a previous analysis of the 77°K absorption spectrum of RNase S (Horwitz and Strickland, 1971). Therefore, the 0–0 bands were placed at 283.5 nm for the three tyrosyls with hydroxy groups available to the solvent (73, 76, 115) and at 286 nm[4] for the three tyrosyl side chains that are hydrogen bonded to other moieties of the protein (Figure 3). These wavelengths were also used to position the degenerate exciton CD components (Tyr-73–Tyr-115, Tyr-92–Tyr-97, Tyr-25–Tyr-97).

The tyrosyl CD spectrum calculated for RNase S (ΣTyr) reliably reproduces the shape of the tyrosyl vibronic structure observed experimentally at 276 and 283 nm (Figure 3). These negative vibronic bands arise primarily from the nondegenerate dipole–dipole coupling between Tyr-73 and Tyr-115. In agreement with the CD spectrum measured for RNase S, the calculated trace lacks obvious vibronic structure at 286 nm, the position of the 0–0 band for Tyr-97, -92, and -25. Even though the CD calculated for Tyr-97 is appreciable, its 0–0 band is obscured by the positive bands from the exciton CD components (Figure 3).

The most obvious difference between the RNase S CD spectrum and the calculated tyrosyl spectrum (ΣTyr) is that the calculated curve has less CD, especially in the region below 270 nm. The total rotatory strength calculated for all tyrosyl side chains (Table IV) is about 55% of the rotatory strength observed experimentally for RNase S between 320 and 250 nm (-20×10^{-40} cgs unit). Some rotatory strength also comes from the phenylalanyl CD bands at 268, 262, and 255 nm (Horwitz *et al.*, 1970; Horwitz and Strickland, 1971). However, measurements based upon the size of these vibronic bands (Strickland *et al.*, 1970a) suggest that the phenylalanyl contribution is only about -0.5×10^{-40} cgs unit. Most of the difference between the RNase S spectrum and the calculated tyrosyl spectrum probably is due to the cystinyl CD bands. A previous analysis of the experimental spectrum suggested that a broad, negative disulfide CD band extends well below 270 nm (Horwitz and Strickland, 1971; Horwitz *et al.*, 1970). The long-wavelength edge of this disulfide CD band can be observed in the RNase S spectrum from 310 to 295 nm, a region where tyrosyls do not have CD bands at 77°K (Figure 3).

In general, disulfide CD bands may arise from inherent dissymmetry and also from interactions with a dissymmetric environment (Linderberg and Michl, 1970). Both mechanisms may be operative in the case of RNase S. Its four disulfide bridges may interact with the surrounding moieties. In addition, the disulfides of RNase S are inherently dissymmetric, having a net negative CD in the long-wavelength region (see Results). This inherent CD band, however, may contribute only a portion of the total disulfide CD of RNase S, since the dihedral angles deviate by only 5 to 15° from +90° or −90° (Table VII). For example, *cyclo*-L-cystine, which has a dihedral angle of 90°, lacks optical activity in its long-wavelength absorption band (Donzel *et al.*, 1972). On the other hand, L-cystine does have a near-ultraviolet CD band (Beychok, 1965; Coleman and Blout, 1968), even though its dihedral angle is near ±90° (Perahia and Pullman, 1971). Interestingly, the $\Delta\epsilon$ value for the long-wavelength band of L-cystine changes from -0.4 M^{-1} cm^{-1} at 293°K to -1.5 M^{-1} cm^{-1} at 77°K, apparently due to increased rigidity (Takagi and Ito, 1972). Evidently the long-wavelength CD band of rigid cystinyl side chains may be appreciable even when the dihedral angle deviates from ±90° by only small amounts (perhaps 5–20°). Similar effects in RNase S may account for its disulfide CD band ($\Delta\epsilon \approx -3$ M^{-1} cm^{-1} at 276 nm, Figure 3).

After correcting for the disulfide and phenylalanyl CD bands of RNase S there is approximate agreement between the experimental RNase S CD spectrum and the tyrosyl spectrum calculated from dipole–dipole coupling. This agreement suggests that the major sources of tyrosyl CD in RNase S have been identified. Fortunately the largest couplings, those between Tyr-73 and Tyr-115, can be evaluated most accurately. The electron densities of Tyr-73 and Tyr-115 are well defined, suggesting that their side chains are fairly rigid in the crystal (Richards and Wyckoff, 1971). Although these side chains are

[4] This wavelength is consistent with the 3.5-nm red shift observed when the hydroxy group of *N*-stearyl-L-tyrosine *n*-hexyl ester is hydrogen bonded to a carbonyl oxygen of an amide (Strickland *et al.*, 1972). Since the hydroxy groups of Tyr-25, -92, and -97 are hydrogen bonded to excellent proton acceptors, their 0–0 bands may be expected at longer wavelengths.

near each other, they are in contact only at their phenolic oxygen atoms (Figure 4F in Wyckoff *et al.*, 1970). Thus the separation of the transition monopoles from the nuclear planes has only a small influence upon the calculated rotatory strength (Table IV). In addition, the interaction energy can be calculated reliably using a dielectric constant of unity, because the region between the phenolic rings of Tyr-73 and -115 is mainly unoccupied.

The only other tyrosyl side chains having appreciable calculated rotatory strengths in RNase S are Tyr-76 and -97 (Table IV). For these weaker CD bands arising mainly from interactions with neighboring peptide bonds, the rotatory strengths could vary by 30–50% for small changes in the atomic coordinates. The rotatory strength calculated for Tyr-97 is especially uncertain, because its side chain is poorly defined in the electron-density maps of crystalline RNase S (Wyckoff *et al.*, 1970). Evidently multiple conformers may exist even in the crystalline state. Thus the conformation in solution or in a glass (77°K) may be different from the proposed X-ray coordinates.

Having evaluated the tyrosyl CD bands resulting from electric dipole–electric dipole coupling, the possible contributions from other mechanisms will be considered. In principle, static perturbations may induce some near-ultraviolet rotatory strength, because each tyrosyl side-chain contacts several peptide bonds or other polar groups (Table V). The actual contribution from this mechanism, however, is probably small. The distribution of perturbing groups does not seem especially favorable for inducing large tyrosyl CD bands (see Results). More importantly, Hooker and Schellman (1970) have reported that static perturbations are an unlikely source for tyrosyl CD.

Optical activity may also arise from coupling of electric dipole transitions on phenolic rings with the magnetic dipole transitions of the disulfide bridges in RNase. R. W. Woody (1971, personal communication) has suggested that this mechanism ($\mu \cdot m$) may give rise to strong disulfide optical activity in the near-ultraviolet region. Since Tyr-73, -115, and -97 are in proximity to disulfide bridges (Table V), their near- or far-ultraviolet transitions may perhaps couple with the magnetic moment of the disulfide transitions. Coupling of this type may be appreciable in RNase S. For gliotoxin, Woody (1971) has found that the near-ultraviolet CD spectrum is dominated by coupling of the diene transition with a disulfide transition.

At this point, let us consider the extent to which the interactions calculated for RNase S apply to RNase A. Unfortunately the structure of crystalline RNase A is not sufficiently well refined to permit calculations of rotatory strengths. At present, the structures of RNase A and S appear similar in most regions, except where the single peptide bond is cleaved in RNase S (Richards and Wyckoff, 1971). Evidently the bond cleaved between residues 20 and 21 causes an altered environment for the Tyr-25 side chain of RNase S, at least in solution, thereby changing its CD and absorption spectra (Horwitz and Strickland, 1971). The calculations for RNase S suggest that the CD intensity of Tyr-25 is sensitive to a local conformation change (see above). Among the remaining tyrosyls of RNase A, it may be anticipated that the interactions between Tyr-73 and Tyr-115 are a major source of rotatory strength. Possibly the tyrosyl–peptide interactions of RNase A differ significantly from those of RNase S, because these rotatory strengths may be altered by even small changes in the atomic coordinates.

The theoretical findings on RNase optical activity have implications for experimental studies based upon pH changes and chemical modification. First, consider some effects of ionizing the "exposed" tyrosyl side chains. At neutral pH's the phenolic oxygen atoms of Tyr-73 and -115 are in contact and appear accessible to the solvent (Wyckoff *et al.*, 1970; Richards and Wyckoff, 1971). After ionization of their phenolic hydroxy groups, these rings will almost certainly be repelled apart and probably will have some motility. Both of these changes would tend to decrease the rotatory strength due to their dipole–dipole coupling. On the other hand, the phenolate side chains would tend to have about 80% more rotatory strength, because the dipole strength of their ^1L_b transitions is 80% larger than that of the phenolic side chains. In addition, ionization of the tyrosyl side chains may possibly affect the CD bands of neighboring disulfides, by means of the $\mu \cdot m$ coupling mechanism, by static perturbations, or perhaps by altering the conformations of the cystinyl side chains. Many of the effects mentioned above may influence the near-ultraviolet CD band of RNase A, when the exposed tyrosyls become ionized; *e.g.*, at pH 11 the CD extremum is shifted to 288 nm and is intensified by 50% (Pflumm and Beychok, 1969; see Simmons and Glazer (1967) for results at pH 11.5).

With chemical modification techniques, it is essential to evaluate if the conformation is altered and to determine which tyrosyl side chains have been modified. Sometimes the "buried" tyrosyl side chains react more rapidly than the "exposed" ones (Myers and Glazer, 1971); *e.g.*, the buried tyrosyls of cytochome *c* are selectively nitrated (Dickerson *et al.*, 1971). The ambiguity of which tyrosyls have been modified may account for some of the conflicting CD spectra of modified RNases. For example, Simons (1971) reported a 50% loss of CD at 275 nm following acylation of three tyrosyls in RNase A, whereas Pflumm and Beychok (1969) found only a 10% loss. Another requirement for interpreting CD spectra is to know the spectral characteristics of the modified side chain. Many modified tyrosyl chromophores have both near- and far-ultraviolet transitions that may couple with π–π^* transitions of unmodified tyrosyls or other protein moieties, thereby creating new optical activity in the near-ultraviolet region.

Acknowledgments

I thank Professor Robert W. Woody for several helpful discussions. His explanations clarified a number of concepts that were essential to this investigation. In addition, I thank Professor H. W. Wyckoff and his coworkers for supplying a revised set of coordinates for crystalline RNase S.

References

Bayley, P. M., Nielsen, E. B., and Schellman, J. A. (1969), *J. Phys. Chem. 73*, 228.

Beychok, S. (1965), *Proc. Nat. Acad. Sci. U. S. 53*, 999.

Chen, A. K., and Woody, R. W. (1971), *J. Amer. Chem. Soc. 93*, 29.

Coleman, D. L., and Blout, E. R. (1968), *J. Amer. Chem. Soc. 90*, 2405.

Dickerson, R. E., Takano, T., Eisenberg, D., Kallai, O. B., Samson, L., Cooper, A., and Margoliash, E. (1971), *J. Biol. Chem. 246*, 1511.

Donzel, B., Kamber, B., Wüthrich, K., and Schwyzer, R. (1972), *Helv. Chim. Acta* (in press).

Gratzer, W. B. (1967), *in* Poly-α-Amino Acids, Vol. 1, Fasman, G. D., Ed., New York, N. Y., Marcel Dekker, p 177.

Hooker, T. M., Jr., and Schellman, J. A. (1970), *Biopolymers 9*, 1319.
Horwitz, J., and Strickland, E. H. (1971), *J. Biol. Chem. 246*, 3749.
Horwitz, J., Strickland, E. H., and Billups, C. (1970), *J. Amer. Chem. Soc. 92*, 2119.
Hsu, M.-C. (1970), Ph.D. Thesis, University of Illinois.
Hsu, M.-C., and Woody, R. W. (1971), *J. Amer. Chem. Soc. 93*, 3515.
Kasha, M (1963), *Radiat. Res. 20*, 55.
Li, L.-K., Riehm, J. P., and Scheraga, H. A. (1966), *Biochemistry 5*, 2043.
Linderberg, J., and Michl, J. (1970), *J. Amer. Chem. Soc. 92*, 2619.
Ludescher, U., and Schwyzer, R. (1971), *Helv. Chim. Acta 54*, 1637.
McDiarmid, R. S. (1965), Ph.D. Thesis, Harvard University,
Meadows, D. H., Jardetzky, O., Epand, R. M., Ruterjans. H. H., and Scheraga, H. A. (1968), *Proc. Nat. Acad. Sci. U. S. 60*, 766.
Myers, B., II., and Glazer, A. N. (1971), *J. Biol. Chem. 246*, 412.
Nielsen, E. B., and Schellman, J. A. (1971), *Biopolymers 10*, 1559.
Paoloni, L. (1959), *Gazz. Chim. Ital. 89*, 957.
Perahia, D., and Pullman, B. (1971), *Biochem. Biophys. Res. Commun. 43*, 65.
Pflumm, M. N., and Beychok, S. (1969), *J. Biol. Chem. 244*, 3973.
Richards, F. M., and Wyckoff, H. W. (1971), *Enzymes 4*, 647.
Schellman, J. A. (1966), *J. Chem. Phys. 44*, 55.
Schellman, J. A. (1968), *Accounts Chem. Res. 1*, 144.
Simmons, N. S., and Glazer, A. N. (1967), *J. Amer. Chem. Soc. 89*, 5040.
Simons, E. R. (1971), *Biochim. Biophys. Acta 251*, 126.
Strickland, E. H., Kay, E., and Shannon, L. M. (1970a), *J. Biol. Chem. 245*, 1233.
Strickland, E. H., Wilchek, M., Horwitz, J., and Billups, C. (1970b), *J. Biol. Chem. 245*, 4168.
Strickland, E. H., Wilchek, M., Horwitz, J., and Billups, C. (1972), *J. Biol. Chem. 247*, 572.
Takagi, T., and Ito, N. (1972), *Biochim. Biophys. Acta 257*, 1.
Tinoco, I., Jr. (1962), *Advan. Chem. Phys. 4*, 113.
Tinoco, I., Jr. (1963), *Radiat. Res. 20*, 133.
Woody, R. W. (1968), *J. Chem. Phys. 49*, 4797.
Woody, R. W. (1971), 162nd National Meeting of the American Chemical Society, Washington, D. C., Sept, Abstract PHYS 110.
Woody, R. W., Friedman, M. E., and Scheraga, H. A. (1966), *Biochemistry 5*, 2034.
Woody, R. W., and Tinoco, I., Jr. (1967), *J. Chem. Phys. 46*, 4927.
Wyckoff, H. W., Hardman, K. D., Allewell, N. M., Inagami, T., Johnson, L. N., and Richards, F. M. (1967), *J. Biol. Chem. 242*, 3984.
Wyckoff, H. W., Tsernoglou, D., Hanson, A. W., Knox, J. R., Lee, B., and Richards, F. M. (1970), *J. Biol. Chem. 245*, 305.

Contribution of Tyrosine to Circular Dichroism Changes Accompanying Neurophysin–Hormone Interaction†

Esther Breslow* and Jane Weis

ABSTRACT: The contribution of changes in tyrosine ellipticity to circular dichroism changes accompanying neurophysin–hormone interaction was assessed by replacing tyrosine-2 of hormone analogs with phenylalanine and by nitrating the single tyrosine of the protein. Substitution of phenylalanine for tyrosine in position 2 of binding peptides led to almost total loss of typical 280-nm ellipticity changes associated with binding, but had little effect elsewhere in the spectrum. Changes in the environment of tyrosine-2 are therefore the major source of the 280-nm ellipticity changes. Nitration of neurophysin had no effect on far-ultraviolet ellipticity changes associated with binding, slightly reduced changes in the 230- to 250-nm region, and led to new ellipticity changes above 300 nm which were attributed to perturbation of the nitrotyrosine. Titration studies indicated that the nitrotyrosine pK was lowered 0.6 pH unit by binding. The effects of binding on the ellipticity and pK of the nitrotyrosine were independent of the nature of the peptide side chain in position 1 and of residues 3–9 when differences in binding affinity were allowed for. These data are interpreted in terms of a model which places the neurophysin tyrosine near the protonated α-amino and the side chain in position 2 of the bound peptide. Of changes elsewhere in the spectrum which accompany interaction of native neurophysin with the hormones, the results further implicate disulfide transitions in ellipticity changes above 291 nm and in the 230- to 250-nm region. Far-ultraviolet changes are tentatively attributed principally to side-chain chromophores.

The specific noncovalent complexes of the neurophysins with oxytocin and vasopressin are of interest not only because of their role in the physiology of the hormones (Sachs, 1969; Sawyer, 1961) but also because they provide useful and accessible models for the study of protein–protein interaction. Studies in this laboratory (Breslow and Abrash, 1966; Bres-

† From The Department of Biochemistry, Cornell University Medical College, New York, New York 10021. *Received March 22, 1972.* Supported by Grant GM-17528 from the National Institutes of Health.

A preliminary report of this work was delivered at the 162nd National Meeting of the American Chemical Society, Washington, D. C., Sept 1971.